

Stability of nanocrystalline Ni-based alloys: coupling Monte Carlo and molecular dynamics simulations

O Waseda^{1,2}, H Goldenstein², G F B Lenz e Silva², A Neiva²,
P Chantrenne¹, J Morthomas¹, M Perez¹, C S Becquart³ and
R G A Veiga⁴

¹ Université de Lyon, INSA-Lyon, MATEIS, UMR CNRS 5510, 25 Avenue Jean Capelle, F-69621, Villeurbanne, France

² Escola Politécnica/Departamento de Engenharia Metalúrgica e de Materiais, Universidade de São Paulo, Av. Prof. Mello de Moraes, 2463, Butantã, CEP 05508-030, São Paulo/SP, Brazil

³ Université de Lille, CNRS, INRA, ENSCL, UMR 8207, UMET, Unité Matériaux et Transformations, F-59000, Lille, France

⁴ Universidade Federal do ABC, Center for Engineering, Modeling, and Social Applied Sciences (CECS), Av. dos Estados, 5001, Santa Terezinha, CEP 09210-580, Santo André/SP, Brazil

E-mail: roberto.veiga@ufabc.edu.br

Received 27 April 2017, revised 28 July 2017

Accepted for publication 3 August 2017

Published 23 August 2017



CrossMark

Abstract

The thermal stability of nanocrystalline Ni due to small additions of Mo or W (up to 1 at%) was investigated in computer simulations by means of a combined Monte Carlo (MC)/molecular dynamics (MD) two-steps approach. In the first step, energy-biased on-lattice MC revealed segregation of the alloying elements to grain boundaries. However, the condition for the thermodynamic stability of these nanocrystalline Ni alloys (zero grain boundary energy) was not fulfilled. Subsequently, MD simulations were carried out for up to 0.5 μ s at 1000 K. At this temperature, grain growth was hindered for minimum global concentrations of 0.5 at% W and 0.7 at% Mo, thus preserving most of the nanocrystalline structure. This is in clear contrast to a pure Ni model system, for which the transformation into a monocrystal was observed in MD simulations within 0.2 μ s at the same temperature. These results suggest that grain boundary segregation of low-soluble alloying elements in low-alloyed systems can produce high-temperature metastable nanocrystalline materials. MD simulations carried out at 1200 K for 1 at% Mo/W showed significant grain boundary migration accompanied by some degree of solute diffusion,

thus providing additional evidence that solute drag mostly contributed to the nanostructure stability observed at lower temperature.

Keywords: segregation, grain growth, nanocrystalline materials, Monte Carlo, molecular dynamics

(Some figures may appear in colour only in the online journal)

1. Introduction

Nanocrystalline materials have attracted the attention of materials scientists in the last decades due to their unique mechanical [1–5], electrical [6, 7], magnetic [8] and corrosion [9, 10] properties. The large deviation of the properties of these materials from those of coarse-grained polycrystals is related to their very fine structure, with grain sizes smaller than 100 nm. There is a wide interest in the applications of these materials, such as in coatings [11, 12], thermoelectrics [13, 14], electronics [15], and also biological and biomedical research [16, 17]. However, owing to the large relative amount of atoms at high energy positions in grain boundaries, this class of nanostructured materials is far from the thermodynamic equilibrium. Therefore, the research for cost-effective alternatives to stabilize the nanometer-sized crystallites has been of scientific and technological interest.

In this work, we focused on nanocrystalline nickel (nc-Ni) as the model system of a nanocrystalline material because of its potential usage in applications requiring high strength and abrasive wear resistance, such as in coatings. Moreover, controlling the size of Ni nanoparticles has been experimentally demonstrated to be important for other advanced applications, such as in nanocomposite-based supercapacitors [18] and catalysis [19]. Electrodeposition [20] and consolidation of nanocrystalline powder [21] are two experimental routes to produce nc-Ni. Pure nanocrystalline metals, however, are known to undergo significant grain growth even at room temperature [22]. This is an important drawback particularly if processing and applications at higher temperatures are envisaged, which is usually the case for nc-Ni. The addition of alloying elements with limited solubility in the metallic matrix is a well-established way of hampering grain migration and growth, thus stabilizing the nanostructure [23–29]. This improvement in the thermal stability is generally associated with the reduction of grain boundary energy through grain boundary segregation [27], although a kinetic contribution from solute drag effect is also expected to take place [30]. Detor and Schuh [31] reported experimental evidence of stable nc-Ni upon alloying with the moderately soluble element W; moreover, they also observed that the amount of W could be used to control the grain size. Analysis of theirs and others' experimental findings [27, 32] suggest that thermodynamics gives a significant contribution to the observed stability of alloyed nanocrystalline systems.

Modeling at different scales has been playing an important role in understanding the effect of alloying on the suppression of grain growth in nanocrystalline systems. Chookajorn and colleagues [33] proposed a thermodynamic model for the design of nanograined materials. Their model was applied to select W-Ti as a candidate, subsequently produced by high-energy ball milling. In a further development, Murdoch and Schuh [34] introduced a 'regular nanocrystalline solution' model taking also into account the problem of phase separation above a certain solute concentration. Liu *et al* [35] employed an empirical model based on thermodynamics that described the stability of the nanocrystalline Fe-P and Ni-P systems, showing a relationship between the solute concentration and the grain size under the condition

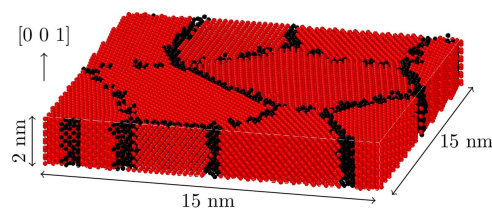


Figure 1. Simulation box: red spheres represent fcc atoms; grain boundary atoms are in black.

of thermodynamic equilibrium. Detor and Schuh [36] presented an insight into the role of alloying on the thermal stability of nc-Ni by means of Monte Carlo (MC) simulations. In their work, the thermal stability of the nanocrystalline Ni-W system was deduced solely from the grain boundary energy decrease due to W segregation. By comparing the simulation results with their own experimental findings, they concluded that the nc-Ni-W alloys were likely to be found in a metastable state in the experiments. In [37], the effect of the atomic size mismatch of segregated solutes on the thermal stability of nanocrystalline Cu alloys was investigated with molecular dynamics (MD) employing simple Lennard-Jones potentials. Pun *et al* [38], in turn, performed semi-grand canonical MC to study the formation of Ta precipitates at grain boundaries in nanocrystalline Cu; thereafter, in MD simulations, those precipitates were able to hinder grain boundary motion through the Zener pinning mechanism, thus preventing grain growth. The interatomic interactions were described by a more sophisticated potential of embedded atom type.

MD is the state-of-the-art technique for atomistic simulations of systems of interest in materials science. However, the time scale that it can achieve is of the order of nanoseconds, even employing the largest parallel machines available nowadays. This is not sufficient to treat segregation, which involves the slow phenomenon of diffusion in the solid state, and therefore the use of other techniques, such as MC, emerges as an alternative. We present in this article a simulation protocol to explore the effect of grain boundary segregation on the stability against grain growth in nc-Ni alloys assuming low concentrations of the alloying elements. Two chemically similar alloying elements were considered: tungsten (W), which was experimentally shown to stabilize nc-Ni [31], and molybdenum (Mo), also commonly utilized as an alloying element in Ni-based alloys. Both are body-centered cubic (Ni is face-centered cubic) high melting point transition metals with similar atomic radius. They also are heavier than Ni. In contrast with W, however, Mo presents very low solubility in fcc Ni at low temperatures. The equilibrium spatial distribution of the alloying elements was estimated using the computationally efficient biased on-lattice MC method previously used to investigate carbon segregation near dislocations in iron [39, 40]. MD simulations of the model systems thus obtained were carried out at high temperature in order to verify whether segregation was able to preserve the nanostructure.

2. Computational approach

2.1. Simulation box and the interatomic potentials

Figure 1 shows the model system, which consisted of nanocrystalline face-centered cubic (fcc) Ni with six randomly oriented columnar grains (i.e., 18 grain boundaries), constructed with Voronoi tessellation and presenting [001] texture along the z -axis. Consequently, the box

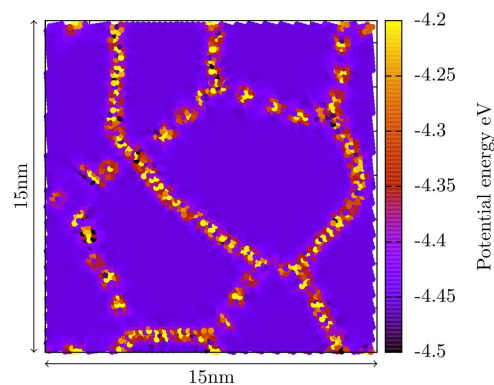


Figure 2. Potential energy of the atoms in the pure nc-Ni system.

contains only tilt boundaries. Periodic boundary conditions are applied in all directions. The volume of the system corresponds approximately to $15 \times 15 \times 2 \text{ nm}^3$ with about 40 000 atoms. The initial structure was equilibrated at 350 K with MD and subsequently its geometry was optimized with conjugate gradient. Next, in order to build the binary alloy models assuming solid solution as the initial system state, atoms of either W or Mo were inserted in the simulation box in the place of randomly chosen Ni atoms up to the desired concentration (ranging from 0.1 to 1 at%). In the corresponding equilibrium diagrams of Ni-W and Ni-Mo, for temperatures above the room temperature and below melting, these solute concentrations are represented on a single phase field for which W and Mo are both in solid solution in the Ni matrix.

The atomic interactions in the MC and MD simulations are described by the Ni-W and Ni-Mo potentials taken from the embedded atom method (EAM) database for alloys introduced in [41]. The potentials in this database were adjusted to reproduce basic properties of the elemental forms and the heat of solution of the alloy systems. The energy calculations required by the MC simulations and the MD simulations were performed by the LAMMPS code [42].

2.2. Biased MC

The biased on-lattice MC algorithm employed in this work is a modified version of the widely used Metropolis–Hastings algorithm [43]. A biased MC simulation proceeds iteratively as follows: 1. Random selection of a position j occupied by an atom of the alloying element (either Mo or W); 2. Selection of a position i occupied by a Ni atom according to the biased probability w_i ; 3. Swapping of the occupations of i and j ; 4. Energy minimization and calculation of the energy of the new state; 5. Acceptance or rejection of the new state according to the acceptance probability p . [39] presents a thorough discussion on this algorithm, addressing particularly the problem of obeying the detailed balance condition. The difference with respect to this work is related to the biased probability. In that reference, carbon atoms were seen to segregate in the vicinity of a screw dislocation, well localized inside the simulation box. Therefore, the bias was applied as a function of the distance of the lattice position from the line defect. This approach is clearly impracticable in the present case.

Figure 2 shows the map of potential energies of the atoms in the pure nc-Ni system. The grain boundary positions can be clearly identified as the regions with the highest energies. The MC algorithm takes advantage of this to speed up the simulations by increasing the

probability of selecting these positions, if occupied by a Ni atom in the alloy system, over bulk positions. The probability w_i of selecting the Ni atom occupying the position i is calculated as $w_i = \exp(\mu E_i)/W$, where μ is the parameter that determines the strength of the bias, E_i is the potential energy associated with position i and $W = \sum_j \exp(\mu E_j)$ normalizes the probability. The value of the parameter μ was set to 20 meV^{-1} in order to have a probability of about 50% of selecting a Ni atom in a grain boundary position. To enforce the detailed balance condition, the bias is compensated at the acceptance/rejection step, as the probability p to accept the new state n is calculated as follows:

$$p(o \rightarrow n) = \min \left[1, \frac{w_o}{w_n} \exp \left(-\frac{E_n - E_o}{k_B T} \right) \right], \quad (1)$$

where w_o and w_n (E_o and E_n) are the selection probabilities (energies) of the old and new states, respectively.

The energy-biased on-lattice MC simulations are performed at 350 K, a typical temperature in electro-deposition experiments [1].

2.3. Molecular dynamics

In this work, the final configurations of the Ni-W and Ni-Mo alloys from the MC simulations were taken as the initial atomic coordinates for the subsequent MD simulations. For all nanocrystalline systems, MD simulations were performed at 1000 K; a few simulations at different temperatures were also performed for verification purposes. The pressure is maintained at zero while the volume of the simulation box was allowed to fluctuate. The MD simulations were performed for up to 500 ns (5×10^8 MD steps, using a timestep of 1 fs). At every 20 ns, a snapshot of the system was taken and its energy was minimized with conjugate gradient in order to determine the state of the grains. The structural evolution of the nano-grained systems in the MD simulations was characterized by the local orientation of every atom obtained from the vectors pointing to its neighbors, taking the fcc unit cell with edges aligned with the x , y and z axes as the reference structure.

3. Results and discussion

3.1. Solubility of the alloying elements in Ni

The interatomic potentials used in this work were not designed for describing intermetallic compounds [41]. This in principle prevents the simulations of high-alloyed Ni-Mo and Ni-W systems that exhibit a variety of ordered structures in their equilibrium diagrams. However, this work is concerned with diluted Ni alloys for which the interatomic potentials are—also in principle—suitable. The maximum concentration of the alloying elements for which the model alloyed systems reasonably reproduce the thermodynamic behavior of the actual alloys was assessed in preliminary simulations.

Molecular statics simulations were carried out for a perfect fcc Ni system with either a single W or Mo atom replacing an Ni atom in the lattice. This simulation box comprised 16 000 atoms. These simulations showed that W and Mo dilution in bulk fcc Ni requires that 0.69 and 0.72 eV, respectively, are absorbed as heat. Such high solvation energies suggest that the interatomic potentials have a tendency for phase separation at relatively low solute concentrations.

Ordinary metropolis MC simulations in the NVT ensemble were performed to determine the limit at which Mo and W can be dissolved in Ni at $T = 350 \text{ K}$ according to the

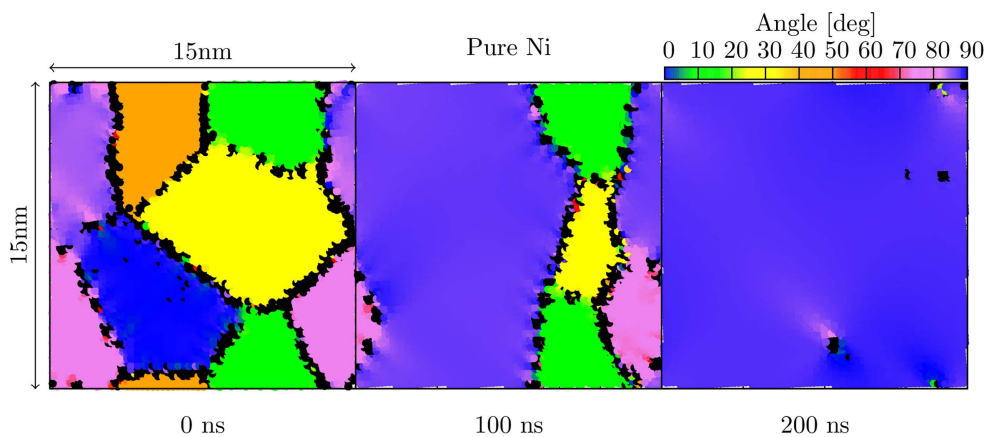


Figure 3. Structural evolution of pure nc-Ni at 1000 K for $t = 0, 100$, and 200 ns.

interatomic potentials. The simulation box consisted of a $12 \times 12 \times 12$ fcc rigid lattice where each site could be occupied by either an Ni atom or a solute atom. The only allowed MC trial move was the random swap of the occupations of two sites occupied by different atomic species. In order to discern between solid solution and phase separation, the occupation probability σ of a site by a solute atom was calculated after MC equilibration for every lattice site in the simulation box. A random solid solution can be characterized by a value of σ approximately equal to the solute concentration in the alloy for most of the lattice sites. Phase separation, in turn, is clearly identified by delimited regions of the simulation box with much higher values of σ . Starting from a high initial concentration of 10 at%, reduced in ensuing MC runs, we observed that for both alloying elements solubilization starts to predominate over phase separation for the same solute concentration of 1 at%, a value close to the actual solubility limit of Mo in Ni but significantly lower than the solubility limit of W in Ni. This value was set as the dilute limit and used as the maximum solute content of this study.

3.2. Thermal instability of nanocrystalline Ni

Preliminary MD simulations were also performed to verify the grain boundary behavior in the pure nc-Ni system depicted in figure 1 as a function of temperature. Pure nanocrystalline metals are known to usually undergo rapid grain growth, but ‘rapid’ in this case may be slow enough to be beyond the reach of MD simulations, particularly at low temperatures. Three annealing temperatures—600, 800 and 1000 K—were considered. Grain boundary migration was observed for the two lowest temperatures, but only at 1000 K grain growth proceeded such that the nc-Ni system transformed entirely into a monocrystal. In total, the grain coarsening process lasted less than 200 ns.

Figure 3 displays the nanostructure evolution of pure nc-Ni at 1000 K. As it can be observed, as grain boundaries started to migrate all grains continuously shrank and ended up disappearing, except one. This last standing grain, initially aligned with the (100) direction and colored in blue, grew at the expense of the other grains and slightly rotated in the course of the MD simulation.

Additionally, MD simulations of nc-Ni with W or Mo in solid solution were carried out also at 1000 K for a concentration of 1 at% of the alloying elements. The kinetics of grain growth was not significantly affected by the presence of solute atoms randomly distributed in

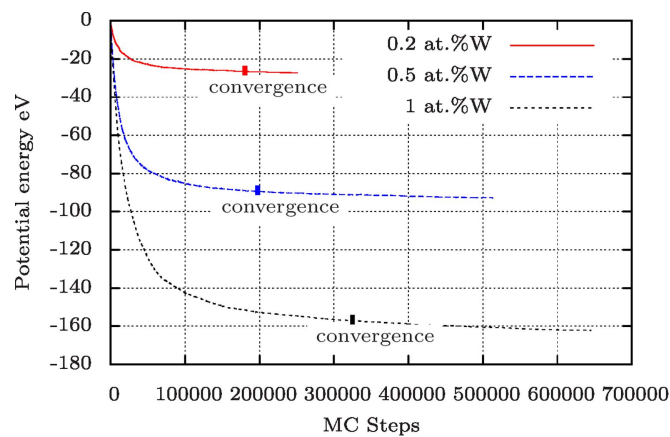


Figure 4. Energy convergence of MC simulations of 0.2, 0.5, and 1.0 at% W.

the grain interiors, proceeding as fast as in pure nc-Ni. This indicates that, at least for such a low solute concentration and high temperature, there is no important drag effect of the migrating grain boundaries as they encounter the solutes on their way.

3.3. Segregation at grain boundaries

On-lattice MC simulations were carried out to estimate the equilibrium spatial distribution of either W or Mo in the corresponding nc-Ni-based alloy. The energy as a function of the number of MC steps N was approximated by a function of form $E(N) = -E_0(1 - \exp(-kN))$, where E_0 is the theoretical energy minimum and k is a parameter, both adjusted to the MC data, and the energy reference is taken as the energy of the random initial configuration. Given the large number of possible configurations for each system (on the order of tens of millions of combinations) and the number of systems to be simulated (20 in total), a compromise between the convergence level and an affordable computing time is necessary. The criterion adopted to determine the energy convergence in the MC algorithm satisfied the condition $\exp(-kN) < 10^{-6}$; for all systems, convergence was usually achieved after a few hundred thousand MC steps. The rigid lattice approach implies that a static microstructure was utilized in the MC simulations, thus the variation in the system energy was solely due to configurational changes in the alloy. Under this condition, the first outcome of the MC simulations is that, for all concentrations of the alloying elements, the energy of the nanocrystalline system was significantly lowered owing to grain boundary segregation. For instance, the evolution of $E(N)$ for nc-Ni-W with 0.2, 0.5, and 1.0 at% W is shown in figure 4; the energy convergence of the MC algorithm is also marked as an eye guide. For these model systems, the energy drop after MC convergence was about 4 meV/atom with an energy difference between the final and the first converged configurations within 0.1 meV/atom. The same applies to nc-Ni-Mo to an equivalent extent.

Figure 5 shows ensemble-averaged local concentration maps of the alloying elements for the systems with 1 at% after MC convergence. In both cases, strong solute segregation is evidenced, with few or even no solute atom remaining in the grain interiors. Enriched grain boundaries consequently exhibit high Mo or W local concentrations, varying from 1.5 to almost 7 at% in the vicinity of triple junctions. It should also be noticed that the grain boundaries were not homogeneously enriched with solute atoms. The nc-Ni model, built with

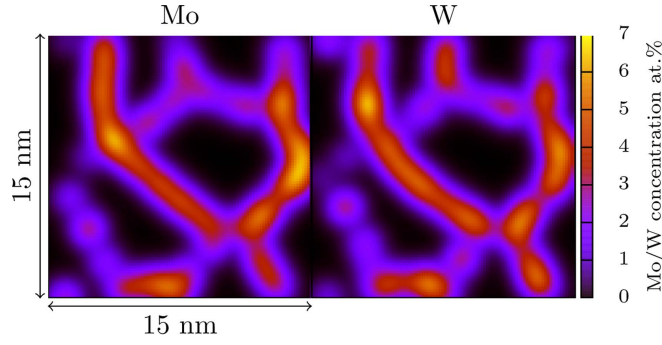


Figure 5. Ensemble-averaged local concentration maps of Mo and W for 1 at% after MC convergence.

random grain orientations, contains low and high angle tilt boundaries: solute enrichment is by far higher for the latter, which have a disordered structure and contain a larger density of high energy positions (as it can be seen in figure 2). On the other hand, regarding the segregation at low angle grain boundaries, the solute enrichment is more pronounced near the core of the grain boundary dislocations.

Voronoi analysis shows that the positions that Mo and W atoms are more likely to occupy after MC convergence are those with the volume of Voronoi cells (a measure of atomic volume) larger than $12 \times 10^{-3} \text{ nm}^3$, found only at grain boundaries; in the grain interiors, perfect (non-strained) fcc positions have a Voronoi cell volume of $11 \times 10^{-3} \text{ nm}^3$. The preference of W and Mo atoms for occupying more open positions at grain boundaries is consistent with the reduction of lattice strain caused by the atomic size misfit. Both alloying elements are substitutionally dissolved in the Ni matrix and, owing to their larger atomic radius (about 0.21 nm, compared to 0.18 nm of Ni), they provoke significant local strain. Conversely, moving Ni atoms from the high-energy miscoordinated grain boundary positions to perfect 12-coordinated fcc positions at grain interiors also contributes to lower the total alloy energy E as observed in the MC simulations. However, the hypothesis for the thermodynamic stability of the nanocrystalline alloys implies that the excess grain boundary energy γ should vanish upon solute segregation. This excess energy for an alloy is calculated as follows:

$$\gamma_x = \frac{\Delta E_{f,x}^{\text{gb}} - \Delta E_{f,x}^{\text{bulk}}}{A}, \quad (2)$$

where $\Delta E_{f,x}^{\text{gb}}$ and $\Delta E_{f,x}^{\text{bulk}}$ are the formation energies of the nanocrystalline alloy and single crystal (bulk) alloy, respectively, for a given composition x of solute, and A is the total grain boundary area. The formation energies, in turn, are given by:

$$\Delta E_{f,x} = E_{\text{alloy}} - (1 - x)E_{\text{Ni}} - xE_{\text{W|Mo}}. \quad (3)$$

In the equation above, E_{alloy} is the per atom energy of either the nanocrystalline alloy or single crystal alloy, whereas E_{Ni} is the per atom energy of fcc Ni and $E_{\text{W|Mo}}$ is the per atom energy of either bcc W or bcc Mo. From equation (2), γ is usually expressed in units of energy per grain boundary area, but obtaining A from the simulation box used in this work is not trivial. Therefore, the grain boundary energy is shown below in units of energy per atom by replacing A by the total number of atoms N .

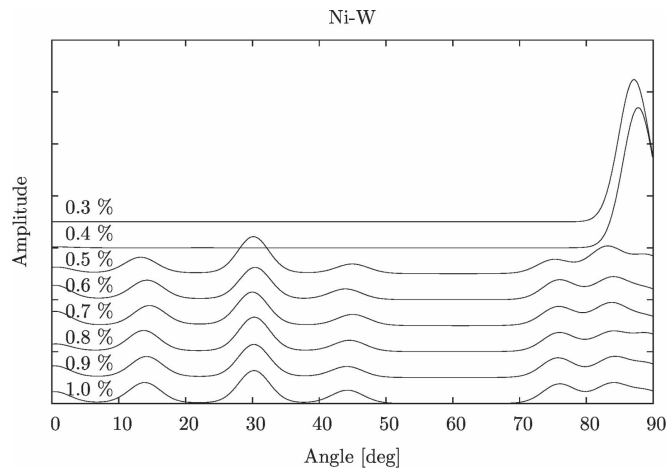


Figure 6. Angle distribution for Ni-W after 500 ns.

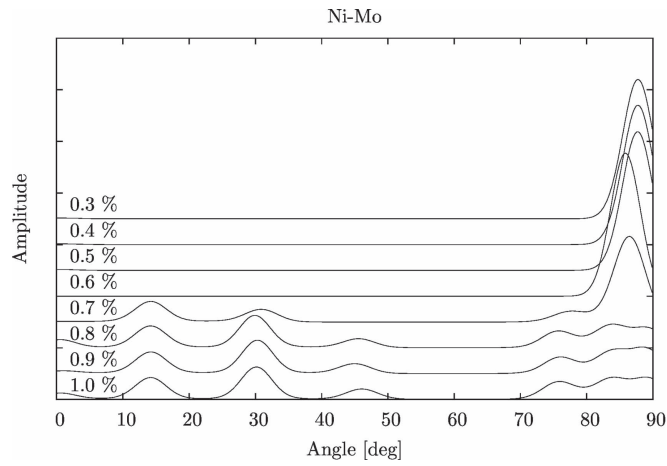


Figure 7. Angle distribution for Ni-Mo after 500 ns.

In the tight concentration range of this study, the values of $\Delta E_{f,x}^{\text{gb}}$ of W and Mo for all the nc-Ni model systems, lying between 24 and 25 meV/atom, were quite similar and almost invariant with respect to the solute concentration. On the other hand, it can be seen that γ decays almost linearly with increasing x for both W and Mo, varying from 23 to 17 meV/atom. Since $\gamma = 33$ meV/atom for $x = 0$, Mo and W segregation effectively reduced the grain boundary energy, but not enough to reach the thermodynamic equilibrium. These results are consistent with the results of the MC simulations—using a different interatomic potential—reported by [36], where the condition for zero grain boundary energy was almost reached only for nc-Ni-W alloys with W contents as high as 40 at%.

3.4. Effect of segregation on grain growth

In the dilute limit considered in this study, W and Mo segregation to grain boundaries in nc-Ni reduced but not eliminated the grain growth driving force related to γ . Another possible

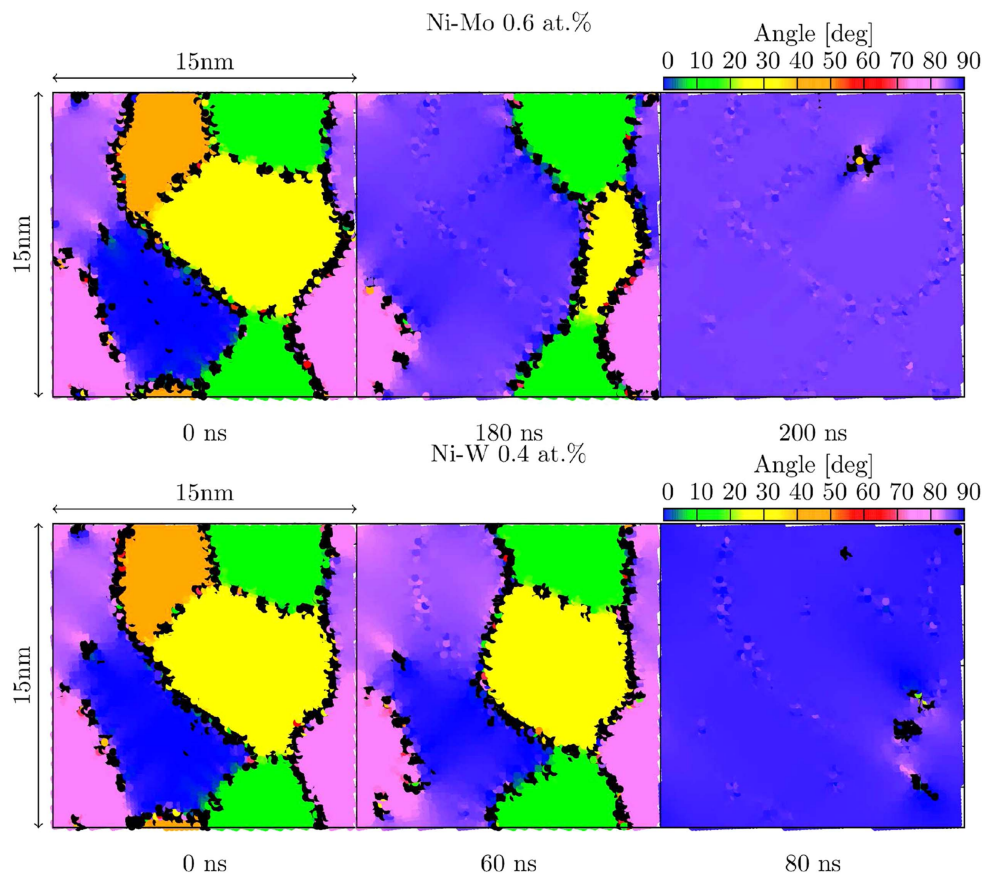


Figure 8. Microstructural evolution of Ni-Mo and Ni-W at 1000 K with 0.6 at% Mo and 0.4 at% W.

contribution to the thermal stability of a nanocrystalline alloy associated with grain boundary segregation is kinetic and arise from the drag effect. The solute load, particularly when comprised of slow diffusing atoms such as substitutional Mo and W, can delay (and virtually stop) grain growth by pinning the grain boundaries. In order to migrate, the grain boundaries have to drag the segregated impurities until, eventually, being able to leave them behind. Next we examine with MD simulations if some of the nanocrystalline systems remain stable at 1000 K due to the additional kinetic contribution coming from the drag effect. As it has been shown above, at this temperature pure nc-Ni and also nc-Ni with W and Mo in solid solution in the grain interiors underwent rapid grain coarsening and transformed into monocrystals.

MD simulations were performed taking the nc-Ni-W and nc-Ni-Mo model systems obtained from converged MC simulations as input coordinates. The effect of segregation on the nanostructure evolution as a function of W and Mo contents at the end of the MD simulations, after 500 ns, can be quantitatively assessed in figures 6 and 7, where the distribution of local atomic tilt angles θ is shown. The peaks in the histograms relate the amount of atoms with the atomic orientations found in the simulation box. The number of these peaks therefore indicate how many grains remained when the MD simulations finished. For W and Mo global concentrations below 0.5 and 0.7 at%, respectively, there is a single peak with

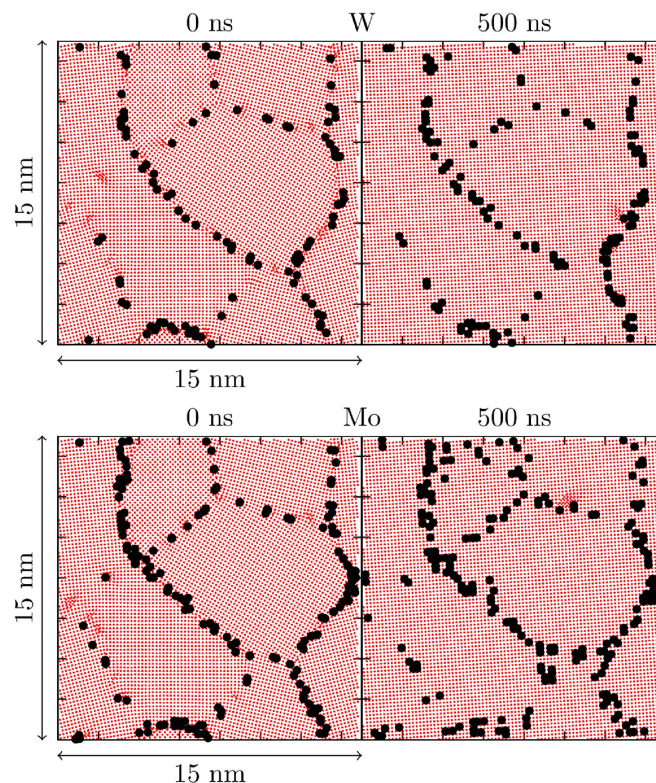


Figure 9. Distribution of W atoms for 0.4 at% and Mo atoms for 0.6 at% in the MD simulations for $t = 0$ and 500 ns.

$\theta \approx 85^\circ$, meaning that solute segregation did not alter the thermal instability of these nc-Ni alloys at 1000 K. In other words, grain growth occurred as in pure Ni and these binary systems also transformed into monocrystals. On the other hand, above these concentration thresholds, some (or all) peaks remain, which implies that grain coarsening was at least partially suppressed and the nanocrystalline structure was mostly preserved.

Figure 8 depicts local atomic orientation maps at different simulation times for the nc-Ni-W with 0.4 at% W and nc-Ni-Mo with 0.6 at% Mo, the maximum global concentrations for which the nanostructure transformed into a monocrystal according to figures 6 and 7. In these alloyed systems, the amount of segregated solutes revealed to be ineffective for pinning the grain boundaries: the beginning of grain growth was somewhat delayed in the case of 0.6 at% Mo, whereas for 0.4 at% W grain boundary migration started even earlier than in the case of pure Ni⁵. In any case, once grain growth initiated, the corresponding nc-Ni alloys evolved into single crystal systems very quickly, after a few tens of nanoseconds. As underpinned by figure 9, this drastic grain growth occurred with some degree of diffusion of the alloying element, with Mo diffusion visually more pronounced than diffusion of heavier W. It can be

⁵ Indeed, rapid grain growth in the model systems can start at any moment during the simulation (but in all cases it started within 200 ns), provided that the amount of segregated solute is not enough to pin the grain boundaries. This is to say that there is some randomness in the beginning (and, indeed, in the speed) of the process. For the sake of illustration, MD simulations performed for 0.4 at% and 0.5 at% Mo, for instance, revealed that grain growth started earlier and proceeded slightly faster for the highest concentration.

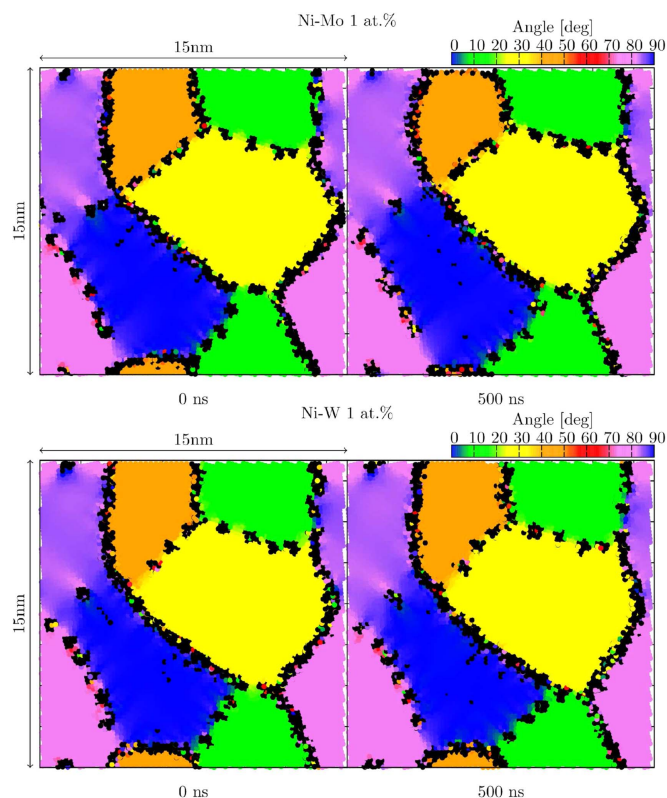


Figure 10. Microstructural evolution of Ni-Mo and Ni-W at 1000 K with 1 at% at the beginning and the end of the MD simulations.

seen that, in the very beginning of grain coarsening, solute atoms moved along with grain boundaries. As soon as the moving grain boundaries finally escaped the slow diffusing solute atoms and were able to migrate faster, the solute-enriched regions left behind constituted a ‘carbon copy’ of the initial nanostructure. On the other hand, figure 10 shows that, although some slight changes in the shape and size of the grains can be seen for 1 at.% of the alloying elements, the nanostructure of the nc-Ni alloys is maintained almost intact if we compare the nanostructures at $t = 0$ and 500 ns. Therefore, despite the thermodynamic driving force for grain growth (i.e., positive grain boundary energy) still holds, it was compensated by the drag force due to the segregated solute atoms.

MD simulations therefore suggest that the addition of small amounts of W or Mo can impede or at least considerably retard grain coarsening in the otherwise thermally unstable nc-Ni model system. In further MD simulations, the temperature was raised to 1200 K for 1 at% W/Mo in order to verify the effect of temperature on the apparent stability against grain growth of these nanocrystalline alloys. Figure 11 shows how both systems evolved after 500 ns. It is evidenced that grain growth occurred in the course of these MD simulations, with one grain completely disappearing while other grains underwent changes in their shape and size. At this higher temperature, Mo and W diffusivities are enhanced, hence the solute atoms tend to spread out and solubilize faster in the alloy. As a consequence, it is easier for the grain boundary to drag the solute atoms as it migrates and eventually breaks free of the solute cloud. These results confirm that the observed stability of the low-alloyed nanocrystalline

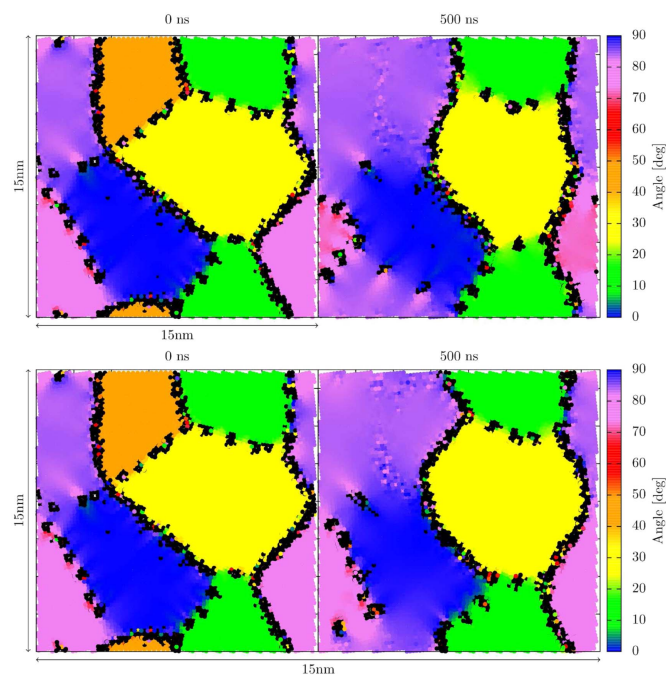


Figure 11. Microstructural evolution of Ni-Mo and Ni-W at 1200 K with 1 at% at the beginning and the end of the MD simulations.

model systems at lower temperature is mostly due to the solute drag effect, depending not only on the amount of segregated solutes but also on the temperature.

4. Conclusions and final remarks

We reported the results of an MC+MD simulation protocol applied to the study of grain boundary segregation of solute atoms in nc-Ni and its effect on the thermal stability of the corresponding alloys. Two chemically similar alloying elements, W and Mo, were substitutionally added in concentrations ranging from 0.1 to 1 at%. Interatomic interactions were described by EAM potentials. Energy biased on-lattice MC simulations were performed at 350 K considering a fixed microstructure to obtain the near-equilibrium states of these binary nanocrystalline systems. The Ni-W and Ni-Mo alloys showed strong segregation of the alloying elements at grain boundaries. Solute segregation reduced, but not to zero, the grain boundary energy. The MC-generated atomic configurations were subsequently used as the initial coordinates in MD simulations. Carried out at 1000 K for up to 0.5 μ s, the MD simulations showed that grain boundary segregation inhibited grain growth in the model systems for minimum global concentrations of 0.5 at% W and 0.7 at% Mo. This is a very different picture from the pure nc-Ni system at the same temperature, for which MD revealed rapid grain growth and the nanocrystalline structure completely transformed into a Ni monocrystal in less than 0.2 μ s. The simulation results therefore suggest that even small additions of W and Mo can stabilize the nanosctrucure of the resulting diluted Ni alloy at high temperatures by means of grain boundary segregation.

For the particular case of Mo as the alloying element, to the authors' knowledge, no experiment on this effect of stabilization of nanocrystalline Ni has been reported so far. The incorporation of computer simulations, particularly at the atomic scale, into the process of designing new materials or improving the properties of existing ones may contribute to reduce the cost and time involved in experiments. Under this perspective, the simulation protocol presented in this work rises as an exploratory methodology that can be used to investigate, with MC, the thermodynamic state and, with MD, the dynamic properties and/or behavior of a wide range of multicomponent engineering materials. Since the theoretical grounds and limitations of MC and MD are well established, the predictability of the modeling technique depends, as usual, on the availability of reliable interatomic potentials.

Acknowledgments

R G A Veiga gratefully acknowledges funding by São Paulo Research Foundation (FAPESP) Young Investigator grant 2014/10294-4. O Waseda was awarded a research scholarship at the University of São Paulo in the framework of the CAPES/COFECUB project 770/13. The authors also acknowledge computing time provided on the Blue Gene/Q supercomputer supported by the Research Computing Support Group (Rice University) and Laboratório de Computação Científica Avançada (Universidade de São Paulo).

References

- [1] Meyers M A, Mishra A and Benson D J 2006 *Prog. Mater. Sci.* **51** 427–556
- [2] Bringa E M, Caro A, Wang Y, Victoria M, McNaney J M, Remington B A, Smith R F, Torralva B R and Van Swygenhoven H 2005 *Science* **309** 1838–41
- [3] Bitzek E, Derlet P, Anderson P and Van Swygenhoven H 2008 *Acta Mater.* **56** 4846–57
- [4] Kumar K, Van Swygenhoven H and Suresh S 2003 *Acta Mater.* **51** 5743–74
- [5] Lund A and Schuh C 2005 *Acta Mater.* **53** 3193–205
- [6] Lu L, Shen Y, Chen X, Qian L and Lu K 2004 *Science* **304** 422–6
- [7] Wang H *et al* 2012 *Nat. Commun.* **3** 917
- [8] Herzer G 2005 *J. Magn. Magn. Mater.* **294** 99–106
- [9] Youssef K M, Koch C and Fedkiw P 2004 *Corros. Sci.* **46** 51–64
- [10] Afshari V and Dehghanian C 2009 *Corros. Sci.* **51** 1844–9
- [11] Jeong D, Erb U, Aust K and Palumbo G 2003 *Scr. Mater.* **48** 1067–72
- [12] Rashidi A and Amadeh A 2008 *Surf. Coat. Technol.* **202** 3772–6
- [13] Wang X *et al* 2008 *Appl. Phys. Lett.* **93** 193121
- [14] da Cruz C A, Katcho N A, Mingo N and Veiga R G 2013 *J. Appl. Phys.* **114** 164310
- [15] Goyal V, Sumant A V, Teweldebrhan D and Balandin A A 2012 *Adv. Funct. Mater.* **22** 1525–30
- [16] Hamad-Schifferli K, Schwartz J J, Santos A T, Zhang S and Jacobson J M 2002 *Nature* **415** 152–5
- [17] Parak W J, Gerion D, Pellegrino T, Zanchet D, Micheel C, Williams S C, Boudreau R, Le Gros M A, Larabell C A and Alivisatos A P 2003 *Nanotechnology* **14** R15
- [18] Zaid N A M and Idris N H 2016 *Sci. Rep.* **6** 32082
- [19] Wang H Y and Lua A C 2012 *J. Phys. Chem. C* **116** 26765–75
- [20] El-Sherik A and Erb U 1995 *J. Mater. Sci.* **30** 5743–9
- [21] Weissmüller J 1996 *Synthesis and Processing of Nanocrystalline Powder* vol 3 (Warrendale, PA: TMS)
- [22] Günther B, Kumpmann A and Kunze H D 1992 *Scr. Metall. Mater.* **27** 833–8
- [23] Averback R, Höfler H and Tao R 1993 *Mater. Sci. Eng. A* **166** 169–77
- [24] Boylan K, Ostrander D, Erb U, Palumbo G and Aust K 1991 *Scr. Metall. Mater.* **25** 2711–6
- [25] Michels A, Krill C, Ehrhardt H, Birringer R and Wu D 1999 *Acta Mater.* **47** 2143–52
- [26] Weissmüller J 1993 *Nanostruct. Mater.* **3** 261–72
- [27] Kirchheim R 2002 *Acta Mater.* **50** 413–9

- [28] Clark B G, Hattar K, Marshall M T, Chookajorn T, Boyce B L and Schuh C A 2016 *JOM* **68** 1625–33
- [29] Li Y, Raabe D, Herbig M, Choi P P, Goto S, Kostka A, Yarita H, Borchers C and Kirchheim R 2014 *Phys. Rev. Lett.* **113** 106104
- [30] Chen Z, Liu F, Wang H, Yang W, Yang G and Zhou Y 2009 *Acta Mater.* **57** 1466–75
- [31] Detor A and Schuh C 2007 *J. Mater. Res.* **22** 3233–48
- [32] da Silva M, Wille C, Klement U, Choi P and Al-Kassab T 2007 *Mater. Sci. Eng. A* **445** 31–9
- [33] Chookajorn T, Murdoch H A and Schuh C A 2012 *Science* **337** 951
- [34] Murdoch H A and Schuh C A 2013 *Acta Mater.* **61** 2121
- [35] Liu F and Kirchheim R 2004 *J. Cryst. Growth* **264** 385–91
- [36] Detor A J and Schuh C A 2007 *Acta Mater.* **55** 4221–32
- [37] Millett P C, Selvam R P and Saxena A 2007 *Acta Mater.* **55** 2329–36
- [38] Pun G P, Darling K, Kecskes L and Mishin Y 2015 *Acta Mater.* **100** 377–91
- [39] Veiga R, Goldenstein H, Perez M and Becquart C 2015 *Scr. Mater.* **108** 19–22
- [40] Waseda O, Veiga R G, Morthomas J, Chantrenne P, Becquart C S, Ribeiro F, Jelea A, Goldenstein H and Perez M 2017 *Scr. Mater.* **129** 16–9
- [41] Zhou X W, Johnson R A and Wadley H N G 2004 *Phys. Rev. B* **69** 144113
- [42] Plimpton S 1995 *J. Comput. Phys.* **117** 1–19
- [43] Frenkel D and Smit B 2001 *Understanding Molecular Simulation: from Algorithms to Applications* (San Diego, CA: Academic)